

ANGULAR DIAMETERS OF THE HYADES GIANTS MEASURED WITH THE CHARA ARRAY

TABETHA S. BOYAJIAN¹, HAROLD A. MCALISTER¹, JUSTIN R. CANTRELL¹, DOUGLAS R. GIES¹, THEO A. TEN BRUMMELAAR², CHRIS FARRINGTON², P. J. GOLDFINGER², LASZLO STURMANN², JUDIT STURMANN², NILS H. TURNER², AND STEPHEN RIDGWAY³

¹ Center for High Angular Resolution Astronomy and Department of Physics and Astronomy, Georgia State University, P.O. Box 4106, Atlanta, GA 30302-4106, USA; tabetha@chara.gsu.edu, hal@chara.gsu.edu, cantrell@chara.gsu.edu, gies@chara.gsu.edu

² The CHARA Array, Mount Wilson Observatory, Mount Wilson, CA 91023, USA; theo@chara-array.org, farrington@chara-array.org, pj@chara-array.org, sturmman@chara-array.org, judit@chara-array.org, nils@chara-array.org

³ National Optical Astronomy Observatory, P.O. Box 26732, Tucson, AZ 85726-6732, USA; sridgway@noao.edu

Received 2008 June 30; accepted 2008 October 5; published 2009 February 2

ABSTRACT

We present angular diameters of the Hyades giants, γ , δ^1 , ϵ , and θ^1 Tau from interferometric measurements with the CHARA Array. Our errors in the limb-darkened angular diameters for these stars are all less than 2%, and in combination with additional observable quantities, we determine the effective temperatures, linear radii, and absolute luminosities for each of these stars. Additionally, stellar masses are inferred from model isochrones to determine the surface gravities. These data show that a new calibration of effective temperatures with errors well under 100 K is now possible from interferometric angular diameters of stars.

Key words: infrared: stars – stars: fundamental parameters – techniques: interferometric

1. INTRODUCTION

Because of its close proximity to the Sun, the Hyades cluster has served as a benchmark in studies ranging from stellar evolutionary modeling to calibrating the cosmic distance scale. In the context of evolutionary theory, *Hipparcos* distances and resolved binaries in the cluster have enabled us to test extensively those models (for example, see Perryman et al. 1998; Lastennet et al. 1999) using fundamental stellar properties such as effective temperature. The only direct way to determine the effective temperature of a star is to measure the star’s angular diameter and integrated flux. While the dwarf stars in the Hyades are too small to resolve their angular diameters with current tools and methods, the four Hyades giants have been observed over the past few decades, beginning with lunar occultation (LO) measurements (see Table 1 for references and timeline of publications of this topic). Presently, long-baseline optical interferometry (LBOI) has trumped LO techniques in accurately measuring the angular diameters of such stars. In fact, for the Hyades giants in particular, the accuracy in the angular diameter measurements has improved by almost an order of magnitude over the past few decades.

In this work, we present the first uniform analysis of all four of the Hyades giants, γ Tau (HR 1346, HD 27371, HIP 20205), δ^1 Tau (HR 1373, HD 27697, HIP 20455), ϵ Tau (HR 1409, HD 28305, HIP 20889), and θ^1 Tau (HR 1411, HD 28307, HIP 20885). We observed these stars with the CHARA Array to obtain their angular diameters to better than 2% accuracy. In combination with the bolometric flux of each star, we derive their effective temperatures to 1% accuracy (Section 3). In this paper, we describe our observational results and then compare them to model isochrones for the Hyades, which demonstrate remarkable agreement within the temperature–luminosity plane for the cluster turnoff age and metallicity (Section 4).

2. OBSERVATIONS AND DATA REDUCTION

We observed these stars with the CHARA Array, located on the grounds of Mount Wilson Observatory, using the CHARA Classic beam combiner in K' band (ten Brummelaar et al. 2005) with the W2-E2 baseline (maximum baseline of 156.3 m) on

2007 November 2 from the Georgia State University Arrington Remote Operations Center (AROC) facility in Atlanta, GA. The chosen calibrator star, δ^2 Tau (HR 1380, HD 27819), an A7V with $v \sin i = 42 \text{ km s}^{-1}$ (Royer et al. 2007), is separated by less than 2 deg on the sky for all of the targets. It was observed in bracketed sequences, with each of the target stars yielding a total of nine bracketed observations for γ , δ^1 , and ϵ Tau, and eight bracketed observations for θ^1 Tau. The angular diameter θ_{SED} of the calibrator star was calculated by fitting observed photometry (see Boyajian et al. 2008 for details) to a model spectral energy distribution (SED).⁴ The close proximity of the Hyades members to us (~ 47 parsecs; van Leeuwen 2007) introduces no effects on the SED fit due to interstellar reddening ($E(B - V) \leq 0.001$ mag, Taylor 2006, and references therein). The SED model fit for the calibrator star yields $\theta_{\text{SED}} = 0.457 \pm 0.020$ mas, for an effective temperature of $T_{\text{eff}} = 8100$ K and $\log g = 4.1$. This corresponds to an absolute calibrated visibility for the calibrator star of ~ 0.97 at these baselines. Data reduction and calibration follow the standard processing routines for CHARA Classic data (as described in ten Brummelaar et al. 2005 and McAlister et al. 2005).

For each calibrated observation, Table 2 lists the time of mid-exposure, the projected baseline B , the orientation of the baseline on the sky ψ , the visibility V , and the 1σ error to the visibility σV for each star.

The duplicity of these stars is not expected to affect our diameter measurements. The secondary stars in these systems are all high contrast in the K band, and our objects are considered as Hyades speckle singles in the infrared K band according to Patience et al. (1998). These nondetections are not surprising. For instance, δ^1 Tau is an SB1 with an M-dwarf companion (Griffin & Gunn 1977) and ϵ Tau is an exoplanet host star (Sato et al. 2007). γ Tau was resolved a single time as a speckle binary (with a large delta magnitude at 5000 Å) by Morgan et al. (1982), having a system separation of 0.395 arcsec. Since this measurement, it has remained undetected as a binary by other programs (McAlister 1978; Mason et al. 1993; Patience

⁴ The model fluxes were interpolated from the grid of models from R. L. Kurucz available at <http://kurucz.cfa.harvard.edu/>.

Table 1
Comparison of Angular Diameter Measurements of the Hyades Giants

γ Tau		δ^1 Tau		ϵ Tau		θ^1 Tau		Method,
$\theta_{LD} \pm \sigma$	$\Delta\theta_{LD}/\sigma_C^a$	$\theta_{LD} \pm \sigma$	$\Delta\theta_{LD}/\sigma_C^a$	$\theta_{LD} \pm \sigma$	$\Delta\theta_{LD}/\sigma_C^a$	$\theta_{LD} \pm \sigma$	$\Delta\theta_{LD}/\sigma_C^a$	Reference
2.91 ± 0.16	-2.4	LO, 1
2.75 ± 0.18	-1.3	LO, 2
...	...	2.97 ± 0.7	-0.8	LO, 3
...	...	2.76 ± 0.7	-0.5	LO, 4
...	2.74 ± 0.12	-3.4	LO, 5
...	1.56 ± 0.45	1.6	LO, 6
...	3.4 ± 1.2	-0.9	LO, 7
...	2.0 ± 0.2	1.5	LO, 8
...	2.8 ± 0.3	-1.6	LO, 9
...	...	2.338 ± 0.033	1.4	2.671 ± 0.032	1.4	Mark III, 10
...	...	2.21 ± 0.08	2.2	2.41 ± 0.11	2.8	NPOI, 11
...	2.57 ± 0.06	2.4	PTI, 12
2.517 ± 0.034	0.0	2.408 ± 0.038	0.0	2.733 ± 0.031	0.0	2.305 ± 0.043	0.0	CHARA, This work

Notes.

^a Here, we define the combined error, $\sigma_C = [\sigma_{CHARA}^2 + \sigma_{Ref}^2]^{0.5}$, where σ_{Ref} is the error to the referenced measurement for each particular star entry. $\Delta\theta_{LD}$ is the difference between our angular diameter and the measurement for each reference.

References. (1) Ridgway et al. 1980; (2) Richichi et al. 1998; (3) Kornilov et al. 1984; (4) Trunkovskij 1987; (5) Ridgway et al. 1982; (6) Radick & Lien 1980; (7) Beavers et al. 1982; (8) Evans & Edwards 1981; (9) White 1979; (10) Mozurkewich et al. 2003; (11) Nordgren et al. 2001; (12) van Belle et al. 1999.

Table 2
Interferometric Measurements of Hyades Giants

Star Name	JD (-2,400,000)	B (m)	ψ (°)	V	σV
γ Tau	54406.745	120.8	194.8	0.495	0.060
γ Tau	54406.770	133.9	195.6	0.393	0.049
γ Tau	54406.784	140.1	196.2	0.391	0.034
γ Tau	54406.799	145.4	197.0	0.382	0.031
γ Tau	54406.822	151.7	198.5	0.413	0.046
γ Tau	54406.842	155.1	200.0	0.321	0.037
γ Tau	54406.861	156.2	201.7	0.350	0.041
γ Tau	54406.884	155.3	204.1	0.377	0.042
γ Tau	54406.913	150.7	207.7	0.355	0.024
δ^1 Tau	54406.752	122.7	193.4	0.504	0.041
δ^1 Tau	54406.776	134.8	194.7	0.507	0.032
δ^1 Tau	54406.793	142.0	195.7	0.447	0.043
δ^1 Tau	54406.819	150.1	197.6	0.410	0.042
δ^1 Tau	54406.846	155.0	199.9	0.368	0.047
δ^1 Tau	54406.865	156.2	201.8	0.395	0.059
δ^1 Tau	54406.874	156.2	202.8	0.356	0.038
δ^1 Tau	54406.897	154.4	205.6	0.380	0.033
δ^1 Tau	54406.925	149.0	209.8	0.403	0.051
ϵ Tau	54406.738	111.5	191.2	0.488	0.058
ϵ Tau	54406.764	126.6	192.7	0.406	0.041
ϵ Tau	54406.781	135.1	193.9	0.330	0.039
ϵ Tau	54406.790	138.8	194.5	0.326	0.038
ϵ Tau	54406.809	145.9	196.0	0.296	0.032
ϵ Tau	54406.833	152.0	198.1	0.246	0.044
ϵ Tau	54406.852	155.0	199.9	0.266	0.031
ϵ Tau	54406.888	155.8	204.1	0.239	0.035
ϵ Tau	54406.909	153.6	207.0	0.260	0.017
θ^1 Tau	54406.758	124.7	194.7	0.546	0.046
θ^1 Tau	54406.802	144.2	196.7	0.462	0.050
θ^1 Tau	54406.812	147.7	197.3	0.414	0.063
θ^1 Tau	54406.836	153.3	199.0	0.439	0.045
θ^1 Tau	54406.855	155.7	200.6	0.438	0.075
θ^1 Tau	54406.871	156.3	202.1	0.382	0.044
θ^1 Tau	54406.900	154.2	205.3	0.430	0.036
θ^1 Tau	54406.919	150.7	207.9	0.444	0.033

et al. 1998). In their infrared speckle program, Patience et al. (1998) did not detect a speckle companion for γ Tau, but placed a limit to the K -band magnitude difference of $\Delta K = 1.04$ for the system. We did not detect a separated fringe packet for the star in any of our observations, and hence we suggest that the detection from Morgan et al. (1982) may be spurious. The speckle binary, θ^1 Tau, is also an SB1 (Torres et al. 1997, and references therein). The companion to θ^1 Tau, is a late F main sequence star (Peterson et al. 1981b), which is supported by the nondetection in Patience et al. (1998), where they list the limiting $\Delta K = 4.6$ magnitudes. As described in Boyajian et al. (2008), our analysis of the binary μ Cas ($\Delta K = 3.5$) shows that the interferometric diameter measured of the primary star of μ Cas is affected by $\sim 1\%$ from the presence of the secondary. Since the magnitude difference in θ^1 Tau is at least one magnitude larger than this system, we neglect any possible influence the secondary star might have on our visibility measurements of the primary star.

3. ANGULAR DIAMETERS AND STELLAR PARAMETERS

The uniform-disk θ_{UD} and limb-darkened θ_{LD} angular diameters are expressed as the following relations:

$$V = \frac{2J_1(x)}{x}, \tag{1}$$

$$V = \left(\frac{1 - \mu_\lambda}{2} + \frac{\mu_\lambda}{3} \right)^{-1} \times \left[(1 - \mu_\lambda) \frac{J_1(x)}{x} + \mu_\lambda \left(\frac{\pi}{2} \right)^{1/2} \frac{J_{3/2}(x)}{x^{3/2}} \right], \tag{2}$$

and

$$x = \pi B \theta \lambda^{-1}, \tag{3}$$

where J_n is the n th order Bessel function, and μ_λ is the linear limb-darkening coefficient at the wavelength of observation.⁵ In

⁵ In this work, we use $\mu_K = 0.301$ for all Hyades giants (Claret et al. 1995).

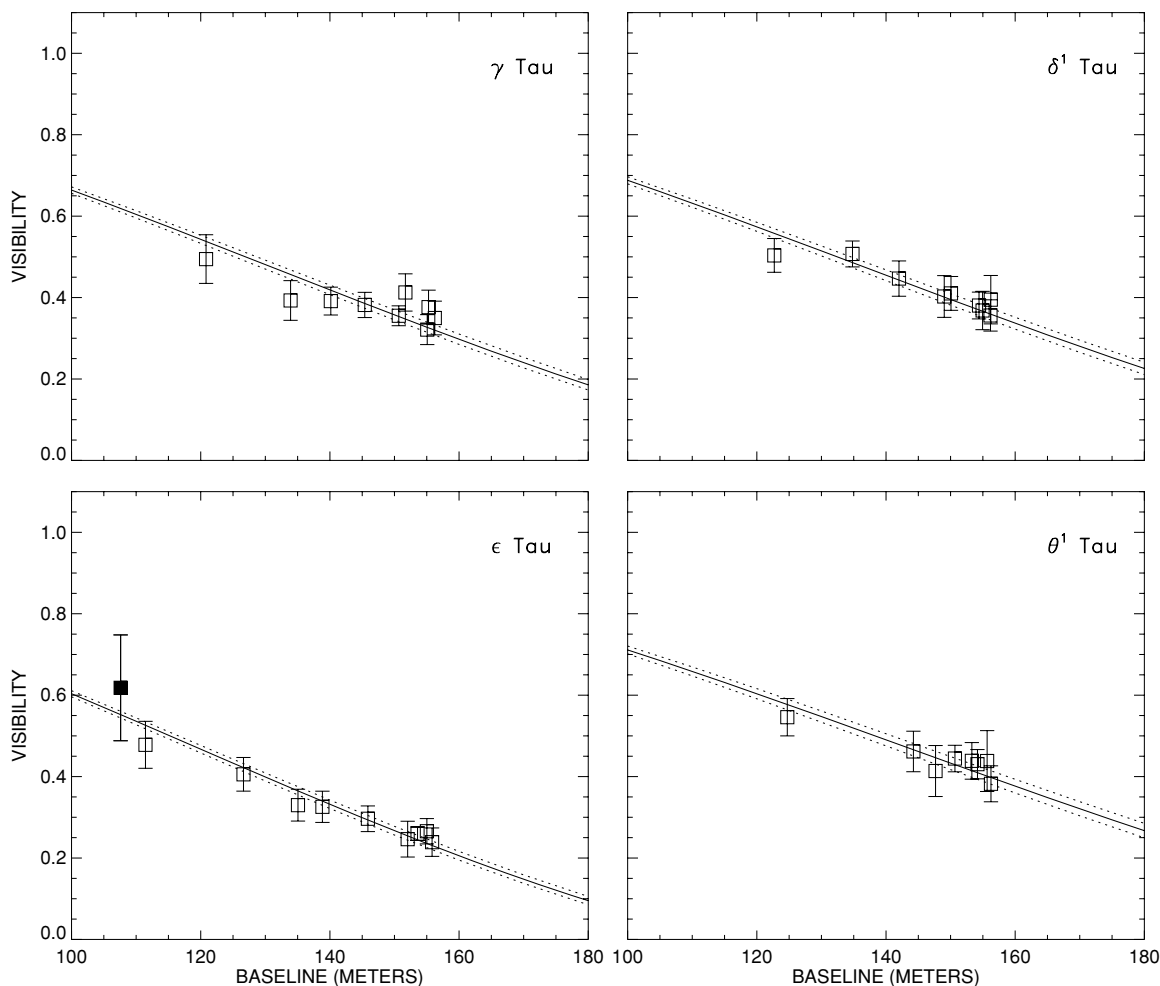


Figure 1. Limb-darkened diameter fits to our data on the Hyades giants. The plot for ϵ Tau also shows the data point from van Belle et al. (1999, filled square).

Table 3
Angular Diameters of Hyades Giants

Star Name	HR	Spectral Type	θ_{UD} (mas)	Reduced χ^2_{UD}	θ_{LD} (mas)	Reduced χ^2_{LD}
γ Tau	HR 1346	K0 III	2.452 ± 0.033	0.88	2.517 ± 0.034	0.86
δ^1 Tau	HR 1373	K0 III	2.347 ± 0.037	0.34	2.408 ± 0.038	0.34
ϵ Tau	HR 1409	G9.5 III	2.660 ± 0.030	0.36	2.734 ± 0.031	0.33
ϵ Tau ^a	HR 1409	G9.5 III	2.659 ± 0.030	0.33	2.733 ± 0.031	0.32
θ^1 Tau	HR 1411	K0 IIIb	2.247 ± 0.042	0.27	2.305 ± 0.043	0.27

Note. ^a Including van Belle et al. (1999) data point.

Table 4
Stellar Properties of Hyades Giants

Star Name	Radius (R_{\odot})	$\log g^a$ (cgs)	F_{BOL}^b ($\text{erg s}^{-1} \text{cm}^{-2}$)	T_{eff} (K)	Range of T_{eff} from Spectroscopy (K)	Range of T_{eff} from Direct Techniques ^c (K)
γ Tau	13.4 ± 0.2	2.58–2.61	116 ± 3	4844 ± 47	4800–4963	4508–4632
δ^1 Tau	12.3 ± 0.4	2.65–2.69	105 ± 3	4826 ± 51	4750–5000	4335–5038
ϵ Tau	13.4 ± 0.2	2.59–2.63	135 ± 4	4827 ± 44	4656–4929	4883–5141
θ^1 Tau	11.7 ± 0.2	2.69–2.73	95 ± 2	4811 ± 50	4874–5000	3962–5842

Notes.

^a Based upon mass range of 2.48–2.70 M_{\odot} .

^b Expressed in $F_{BOL}/1E - 8$. To correct for the light from the secondary component of θ^1 Tau, a 3% reduction to F_{BOL} was applied (Torres et al. 1997; Peterson et al. 1981a, 1981b).

^c Includes the LO- and the LBOI-measured angular diameters, when available (see Table 1).

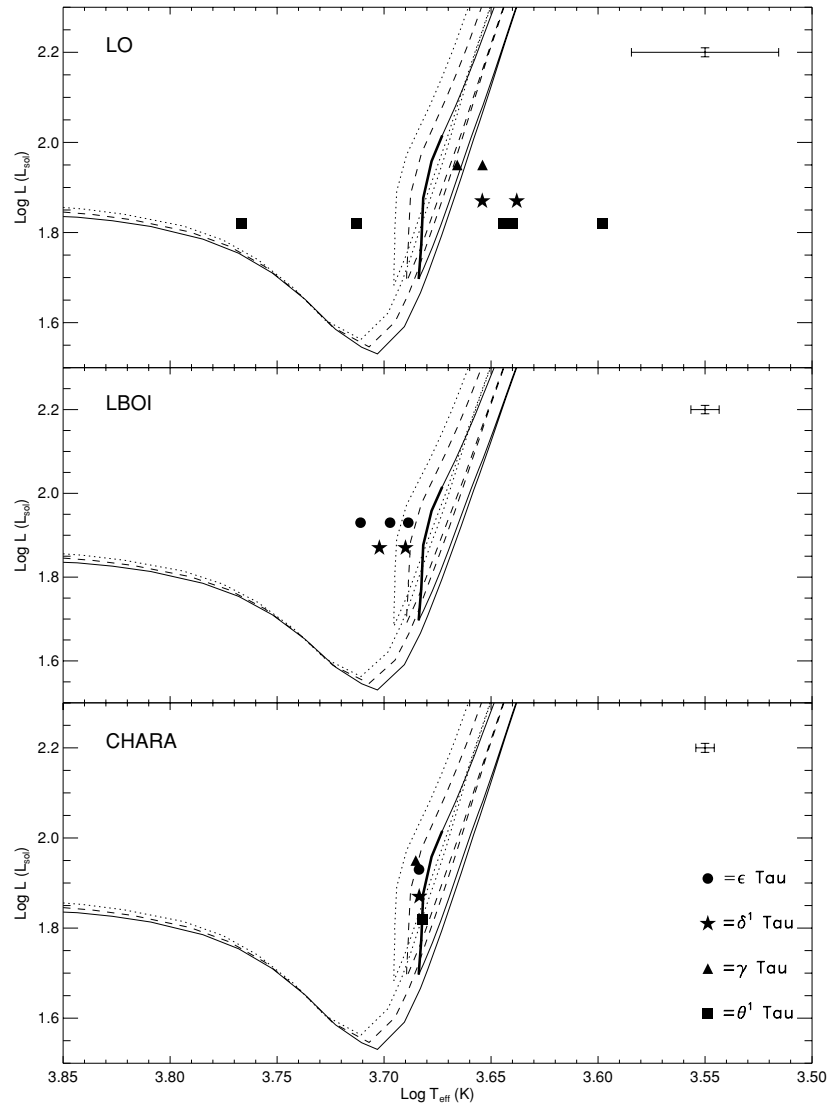


Figure 2. Effective temperatures derived from published angular diameter data from LO (top panel), previous LBOI (middle panel), and this work (bottom panel). The symbols denoting the objects are consistent within all three panels, and the references for each measurements can be found in Table 1. The typical 1σ error for each method is shown in the top right portion of each panel. Padova model isochrones for 625 Myr are plotted for solar metallicity $Z_{\odot} = 0.019$ (dotted line) and metallicities $Z = 0.024$ and $Z = 0.028$ (dashed line and solid line, respectively). The thick region of the Hyades isochrone for $Z = 0.028$ identifies the region of the helium burning RC.

Equation (3), B is the projected baseline in the sky, θ is the UD angular diameter of the star when applied to Equation (1) and the LD angular diameter when used in Equation (2), and λ is the central wavelength of the observational bandpass (Hanbury Brown et al. 1974).

We calculate the UD and LD diameters for each star from the calibrated visibilities by χ^2 minimization of Equations (1) and (2), where the error to the diameter fit is based upon the values on either side of the minimum for which $\chi^2 = \chi_{\min}^2 + 1$ (Press et al. 1992; Wall & Jenkins 2003). Table 3 shows our results along with the reduced χ^2 values for these diameter fits. Note that our values for reduced χ^2 are less than 1, meaning we have overestimated the errors of the measured visibilities used in the diameter fits (σV in Table 2). The best fits for the limb-darkened angular diameters to our calibrated visibilities and the 1σ errors are shown in Figure 1. In our final analysis of ϵ Tau, we include the data point from van Belle et al. (1999), which was taken at the same wavelength as our observations, in the fit.

The angular diameters of these stars are then transformed into linear radii R using the van Leeuwen (2007) *Hipparcos*

parallaxes. In addition to these quantities, we calculate the effective temperature T_{eff} using the relation

$$F_{\text{BOL}} = \frac{1}{4} \theta_{\text{LD}}^2 \sigma T_{\text{eff}}^4, \quad (4)$$

where σ is the Stefan–Boltzmann constant.

The bolometric flux F_{BOL} for each star was determined by applying the bolometric corrections of each star from Allende Prieto & Lambert (1999), assuming $M_{\text{BOL},\odot} = 4.74$. The results for the radius, bolometric flux, and effective temperature for each star are shown in Table 4. The significance of the luminosity subclass IIIb for θ^1 Tau (Table 3) is directly detected here in the smaller radius and F_{BOL} compared to the other giants.

4. DISCUSSION

Historically, each of these stars has been observed by LO and/or LBOI to obtain angular diameters (Table 1). Diameters of three of the four giants have been measured by LO, and somewhat surprisingly, only two of the four giants had been

measured by LBOI prior to this work. While the LO measurements show a considerable scatter and large errors, the LBOI points also vary considerably within their errors with respect to each other. Indeed, this is primarily an artifact of the relatively small size of these four stars creating quite a challenge for them to be sufficiently resolved with interferometers of modest baselines. The advantages of observing stellar diameters with the long baselines of the CHARA Array are apparent, allowing us to obtain optimal sampling of the visibility curve. For example, our measured diameter of ϵ Tau here includes the single PTI data point (Table 3 and Figure 1), clearly improving the diameter fit from van Belle et al. (1999; see Table 1). Secondly, the sensitivity of our beam combiner allows us to observe calibrator stars that are very unresolved, closing the gap for systematic errors that may arise in the calibration process. Additionally, these observations were made in the infrared, and are less subject to stellar limb darkening, making the transformations from the observed θ_{UD} to the actual θ_{LD} less model-dependent.

For all existing angular diameter measurements from LO and LBOI (Table 1), we use Equation (1) to calculate the effective temperatures of these stars (Table 4, Direct Techniques). For comparison, we show the range in effective temperature determinations when estimated via photometric and spectroscopic methods (Ochsenbein et al. 2000), also in Table 4. Our temperatures tend to lie on the low side of these ranges, which probably results from differences in model opacities and varying metallicity determinations of the models used in each reference. In the case of θ^1 Tau, the temperatures from spectroscopic techniques are higher than our derived temperature, which is likely to be an artifact of the duplicity of the star.

Figure 2 displays these available measurements on an H–R diagram for all stars, separated by the method of measurement. To model these stars, we use the Padova database of stellar evolutionary tracks and isochrones⁶ (Marigo et al. 2008), using a cluster turnoff age of 625 Myr (Perryman et al. 1998). In Figure 2, we show isochrones for solar metallicity $Z_{\odot} = 0.019$ and two different metallicities of the Hyades $Z_{\text{Hyades}} = 0.024, 0.028$ (Perryman et al. 1998; Thevenin 1998). The model isochrone for both Hyades metallicities ($Z_{\text{Hyades}} = 0.028, 0.024$) are in excellent agreement with our observations. To identify which part of this isochrone our stars were likely to lie, we investigated a single-star evolutionary track for a mass of $2.5 M_{\odot}$ to determine which part of the isochrone a star would spend most of its lifetime (Girardi et al. 2000). We find that from the beginning of the core helium burning stage, up until the time helium is exhausted from the core, corresponds to $\sim 20\%$ of the stars' total lifetime, second only to the time spent on the main sequence, $\sim 75\%$ of its total lifetime. The stars' placement on Figure 2 clearly mark all four giants as residing on the helium burning red clump (RC), and this region is indicated as the thicker part of the Hyades metallicity isochrone of $Z_{\text{Hyades}} = 0.028$.

Within this region of the RC, we look back to the model isochrones in order to determine a range of masses that these stars may have. The model stellar mass for the lowest point of the RC is $2.48 M_{\odot}$, and following this track up the end of the helium burning stage extends this model mass to $2.70 M_{\odot}$. These masses are consistent with the Torres et al. (1997) giant masses for the Hyades. Assuming that these stars may fall anywhere between these masses, we predict a $\log g$ using the

radii that we measure for each star (Table 4). These values are in excellent agreement with spectroscopically determined gravities found in the literature which have a large spread of values from $\log g = 2.2$ to $\log g = 3.17$, although for most estimates the gravity agrees with ours within 0.1 dex.

We thank Gerard T. van Belle for his advice on the data analysis. The CHARA Array is funded by the National Science Foundation through NSF grant AST-0606958 and by Georgia State University through the College of Arts and Sciences. This research has made use of the SIMBAD literature database, operated at CDS, Strasbourg, France, and of NASA's Astrophysics Data System. This publication makes use of data products from the Two Micron All Sky Survey (2MASS), which is a joint project of the University of Massachusetts and the Infrared Processing and Analysis Center/California Institute of Technology, funded by the National Aeronautics and Space Administration and the National Science Foundation.

REFERENCES

- Allende Prieto, C., & Lambert, D. L. 1999, *A&A*, 352, 555
 Beavers, W. I., Cadmus, R. R., & Eitter, J. J. 1982, *AJ*, 87, 818
 Boyajian, T. S., et al. 2008, *ApJ*, 683, 424
 Claret, A., Diaz-Cordoves, J., & Gimenez, A. 1995, *A&AS*, 114, 247
 Evans, D. S., & Edwards, D. A. 1981, *AJ*, 86, 1277
 Girardi, L., Bressan, A., Bertelli, G., & Chiosi, C. 2000, *A&AS*, 141, 371
 Griffin, R. F., & Gunn, J. E. 1977, *AJ*, 82, 176
 Hanbury Brown, R. H., Davis, J., Lake, R. J. W., & Thompson, R. J. 1974, *MNRAS*, 167, 475
 Kornilov, V. G., Mironov, A. V., Trunkovskii, E. M., Khaliullin, K. F., & Cherepashchuk, A. M. 1984, *Sov. Astron.*, 28, 431
 Lastennet, E., Valls-Gabaud, D., Lejeune, T., & Oblak, E. 1999, *A&A*, 349, 485
 Marigo, P., Girardi, L., Bressan, A., Groenewegen, M. A. T., Silva, L., & Granato, G. L. 2008, *A&A*, 482, 883
 Mason, B. D., McAlister, H. A., Hartkopf, W. I., & Bagnuolo, Jr., W. G. 1993, *AJ*, 105, 220
 McAlister, H. A. 1978, *PASP*, 90, 288
 McAlister, H. A., et al. 2005, *ApJ*, 628, 439
 Morgan, B. L., Beckmann, G. K., Scaddan, R. J., & Vine, H. A. 1982, *MNRAS*, 198, 817
 Mozurkewich, D., et al. 2003, *AJ*, 126, 2502
 Nordgren, T. E., Sudol, J. J., & Mozurkewich, D. 2001, *AJ*, 122, 2707
 Ochsenbein, F., Bauer, P., & Marcout, J. 2000, *A&AS*, 143, 23
 Patience, J., Ghez, A. M., Reid, I. N., Weinberger, A. J., & Matthews, K. 1998, *AJ*, 115, 1972
 Perryman, M. A. C., et al. 1998, *A&A*, 331, 81
 Peterson, D. M., Baron, R. L., Dunham, E., & Mink, D. 1981a, *AJ*, 86, 1090
 Peterson, D. M., Baron, R. L., Dunham, E., Mink, D., Elliot, J. L., & Weekes, T. C. 1981b, *AJ*, 86, 280
 Press, W. H., Teukolsky, S. A., Vetterling, W. T., & Flannery, B. P. 1992, *Numerical Recipes in C. The Art of Scientific Computing*, (2nd ed.; Cambridge: Cambridge Univ. Press)
 Radick, R., & Lien, D. 1980, *AJ*, 85, 1053
 Richichi, A., Ragland, S., Stecklum, B., & Leinert, C. 1998, *A&A*, 338, 527
 Ridgway, S. T., Jacoby, G. H., Joyce, R. R., Siegel, M. J., & Wells, D. C. 1982, *AJ*, 87, 808
 Ridgway, S. T., Jacoby, G. H., Joyce, R. R., & Wells, D. C. 1980, *AJ*, 85, 1496
 Royer, F., Zorec, J., & Gómez, A. E. 2007, *A&A*, 463, 671
 Sato, B., et al. 2007, *ApJ*, 661, 527
 Taylor, B. J. 2006, *AJ*, 132, 2453
 ten Brummelaar, T. A., et al. 2005, *ApJ*, 628, 453
 Thevenin, F. 1998, *VizieR Online Data Catalog*, 3193, 0
 Torres, G., Stefanik, R. P., & Latham, D. W. 1997, *ApJ*, 485, 167
 Trunkovskij, E. M. 1987, *Sov. Astron. Lett.*, 13, 379
 van Belle, G. T., et al. 1999, *AJ*, 117, 521
 van Leeuwen, F. 2007, *Hipparcos, the New Reduction of the Raw Data*, Cambridge Univ. Series: Astrophysics and Space Science Library 350 (Cambridge, UK: Institute of Astronomy), 20
 Wall, J. V., & Jenkins, C. R. 2003, *Practical Statistics for Astronomers* (Princeton Series in Astrophysics)
 White, N. M. 1979, *AJ*, 84, 872

⁶ <http://stev.oapd.inaf.it/cmd>